Measurement of deuteron- and proton-induced Lithium reaction cross sections for SLICS detector efficiency calibration

Mark Yuly, Andrew Bo, Sam Plymale, Dante Vara, Charlie Freeman, George Marcus, Stephen Padalino.

I. The Short-lived Isotope Counting System (SLICS)

The Short-lived Isotope Counting System (SLICS) was developed over the past nine years [1-, 2, 3, 4, 5, 6, 7, 8, 9, 10, 11,12] to detect the radioactive reaction products produced in laser-driven activation experiments involving light ions, of both the Inertial Confinement Fusion (ICF) and Target Normal Sheath Acceleration (TNSA) type. The detector, which consists of a dE-E phoswich plastic scintillator detector and associated high-speed readout electronics, has been tested in previous OMEGA-60 ride-along experiments [6, 7, 8], in experiments [9, 10] to trap and count radioactive reaction products in a simulated-ICF neutral expanding gas, and in a TNSA experiment [10, 11] using the Multi-Terawatt laser (MTW) to accelerate deuterons to produce and detect ^{8}Li via the ^{7}Li(d,p)^{8}Li reaction. During the summer of 2024, in order to test the efficiency predicted by a GEANT simulation for ^{8}Li, an efficiency measurement was carried out at SUNY Geneseo (Figure 1), as well as ride along OMEGA-60 experiments to measure the ^{8}Li produced by ^{11}B(n,α)^{8}Li and the ^{6}He produced by ^{9}Be(n,α)^{6}He by primary ICF neutrons from a high-yield DT shots [12].

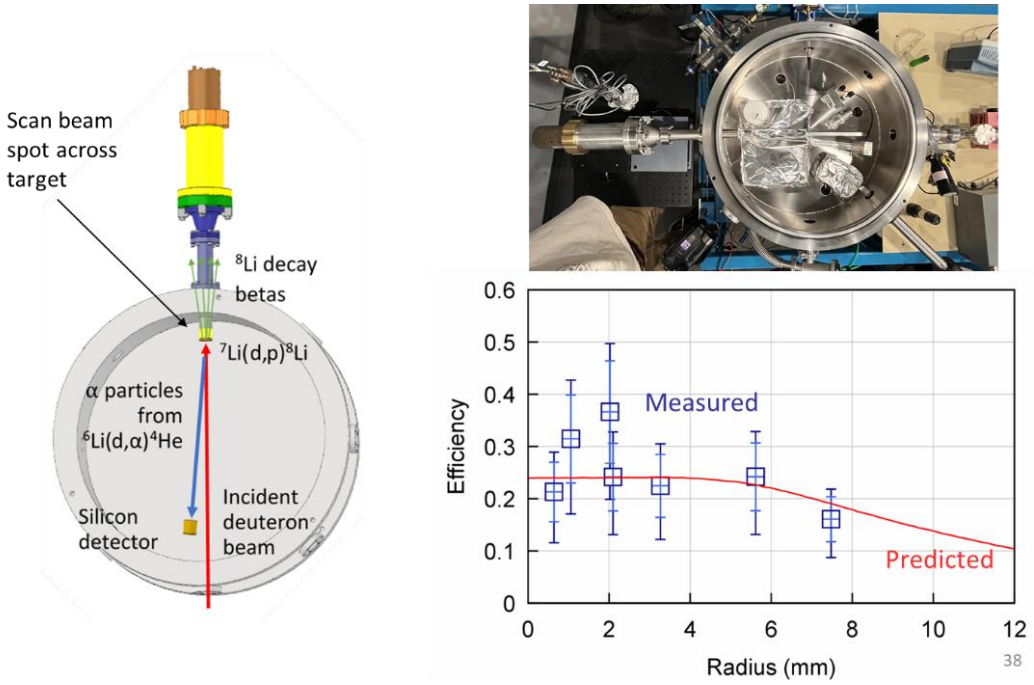

Figure 1. (Left) The deuteron beam entered the chamber and struck the lithium film on the end of the SLICS detector, which detected beta particles from the decay of ^{8}Li created by ^{7}Li(d,p)^{8}Li. The efficiency was measured at several locations on the face of the lithium target by scanning the deuteron beam to several radius settings. The beam current was measured several times throughout the experiment using the well-known ^{197}Au(d,d)^{197}Au elastic scattering cross section and monitored using alpha particles from the ^{6}Li(d,α)^{4}He reaction scatter at 173.4° into the 500 mm^{2} silicon detector. (Right top) A photograph of the scattering chamber showing SLICS, the lithium target, and the silicon detector. (Right bottom). The efficiency predicted by the Geant4 simulation (red) compared to the measured (blue squares) efficiency as a function of distance from the center of the detector face. The error bars indicate the range in efficiency due to the range of possible target thickness (dark blue) resulting from the spread in measured Li(d, p)^{8}Li and ^{7}Li(p, α)^{4}Hecross sections, and the range of possible ^{7}Li(d,p)^{8}Li cross sections at 1.5 MeV (light blue).

In the efficiency measurement at SUNY Geneseo, 1.5 MeV deuterons were allowed to strike a point on a natural lithium target just upstream of the SLICS detector, creating ^{8}Li via the ^{7}Li(d,p)^{8}Li reaction. The number of detected beta decays (N_D) were then counted, and were used, along with the predicted number of ^{8}Li created by the ^{7}Li(d,p)^{8}Li reaction (N_{8Li}), to determine the efficiency $e = N_D/N_{8Li}$. In order to do this, however, accurate measurements of the ^{6}Li(d, p)^{8}Li, ^{7}Li(p, α)^{4}He, and ^{6}Li(d, α)^{4}He cross sections were needed; cross sections which, especially for proton-induced reactions, have been called into question [13]. This report describes an attempt to measure these cross sections that was made in the summer of 2025 using the SUNY Geneseo Pelletron.

II. Experiment Design

The experiment was carried out by Houghton University and SUNY Geneseo students and faculty (Figure 2) to measure the desired ^{6}Li(d, p)^{8}Li, ^{7}Li(p, α)^{4}He, and ^{6}Li(d, α)^{4}He reaction cross sections using the 1.7 MV Tandem Pelletron accelerator at SUNY Geneseo. An approximately 1-6 nA beam of protons or deuterons of energies 1.5 MeV, 1.3 MeV or 1.1 MeV was allowed to strike a thin lithium target on a 116 nm thick gold substrate as shown in Figure 3. The plane of the target was placed at an angle of 59° with respect to the beam, and oriented so that the incident ions struck the gold foil first, then entered the lithium where they scattered elastically or inelastically or caused other nuclear reactions. The scattered particles were detected by two detectors: (1) a 50 mm^2 silicon detector ("RBG") of thickness 300 μm positioned 63 mm from the target on a moveable arm, and (2) a 50 mm^2 silicon detector ("RBS") of thickness 500 μm positioned 105 mm from the target at a fixed angle of 166°. Data were collected for the RBG detector angles of 40°, 60°, 90°, 120°, 140°, 160°, and an RBS detector angle of 166°.

Figure 2. (Left) The accelerator control room operators were Dr. Freeman and students Sam Plymale and Michelle Woods. (Center and Right) Houghton University students Dante Vara and Sam Plymale worked on setup and data analysis.

In order to measure cross sections, it was necessary to know both the beam current and the areal density of both ^{6}Li and ^{7}Li in the lithium target. Since the thickness of the gold foil has been previously measured, it can be used to determine the beam current using the well-known cross section for elastic scattering from gold. For this the screened Rutherford cross section described in Ref. [14] was used, with corrections for low-energy partial screening of the nuclear charges by the electron shell (L'Ecuyer screening) and corrections to this for forward angles (Anderson screening). The resulting cross sections should be accurate to within a few percent.

Once the beam current was determined for each angle and energy setting, elastic scattering from ^{6}Li and ^{7}Li was used to calculate the areal density of each isotope using the same Rutherford scattering formulation. These areal densities, plus the beam current, were then used to calculate the cross sections of the other reactions.

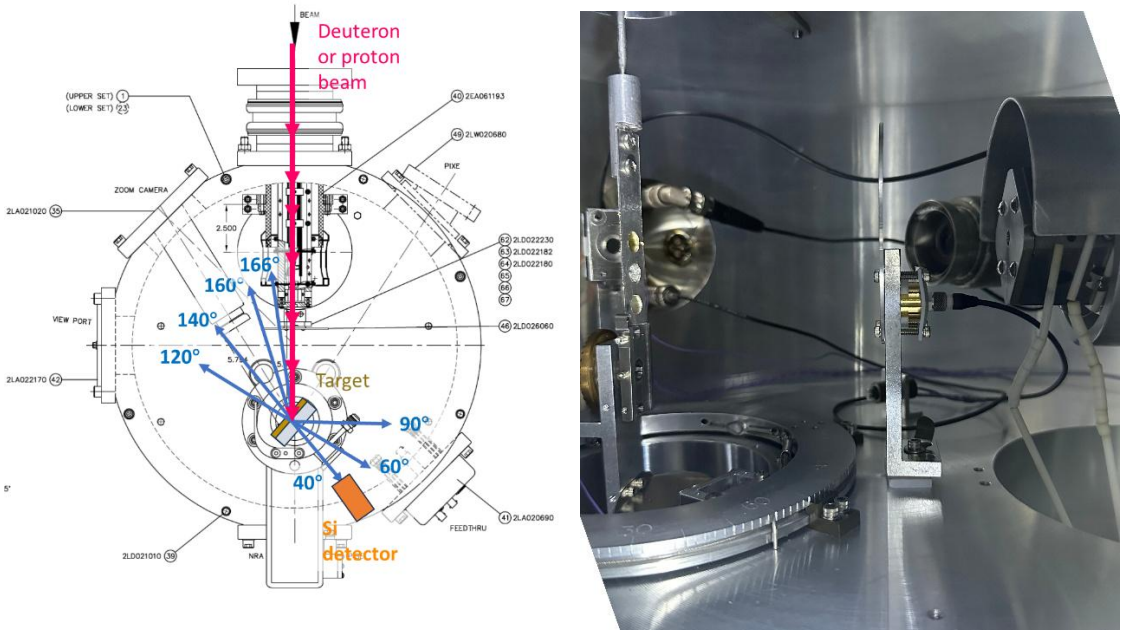

Figure 3. (Left) Layout of the experimental setup in the 15R scattering chamber. Protons or deuterons from the accelerator struck a lithium coated gold foil and scattered elastically or initiated nuclear reactions. The outgoing particles were detected by two silicon detectors at several angle settings. (Right) Photograph of the interior of the scattering chamber, showing the target foil and the two silicon detectors (one is located behind the target and one directly upstream of the target). Two cameras allowed the target foil and the detector to be accurately positioned.

III. Lithium Targets

Clearly, very thin lithium targets were needed to carry out this measurement, in order to reduce the energy loss and spread in energy of the scattered particles and allow them to be identified by their peaks in the energy spectrum. A 1.5 MeV deuteron will lose only about 0.015 MeV/μm in lithium, whereas in gold the rate is 0.14 MeV/μm. Figure 4 shows the predicted outgoing ion energies for each of the reactions of interest for both incident protons and deuterons. It is clear that the separation between the ^{6}Li and ^{7}Li elastic scattering peaks is at most a few hundred keV, and that at forward angles the gold and lithium elastic peaks will converge. In order to limit the energy loss as much as possible and still allow for both transmission and backscattering geometries, the target was created by vacuum vapor deposition of a few μm of natural lithium onto a 116 nm thick self-supporting gold substrate, resulting in an energy loss of only 0.16 MeV for 1.5 MeV deuterons in the gold foil, and 0.15 MeV loss if the target was 10 μm of lithium.

Lithium reacts strongly in humid air to form a number of different compounds, such as lithium hydroxide and lithium nitride. When left out for more than a few minutes, it will eventually all become white lithium oxide. Since the presence of other elements like oxygen, nitrogen and hydrogen other than just gold and lithium would create other peaks in the energy spectrum, most likely obscuring the ones of interest, a special target "airlock" system was created to keep the target in vacuum, as shown in Figure 5.

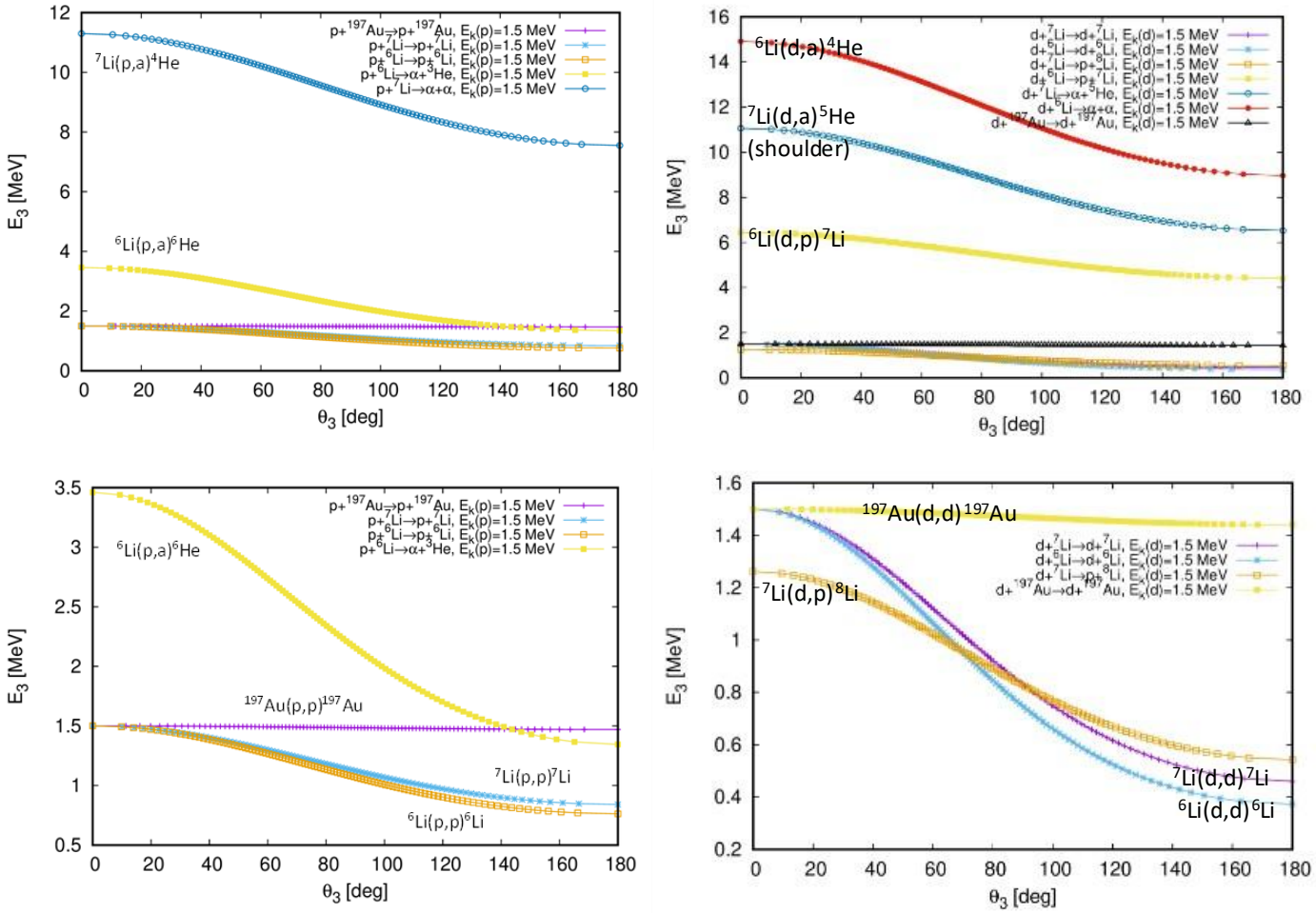

Figure 4. Energy of the outgoing ion as a function of scattering angle for elastic scattering from gold and lithium, as well as the other nuclear reactions of interest for 1.5 MeV protons (left column) and deuterons (right column). For each projectile, the lower plot shows the energy difference between elastic scattering from ^{6}Li and ^{7}Li.

The airlock system consists of a home-made vacuum motion feedthrough that allows both rotation and a very long distance translation of almost 70 cm. This allows a small aluminum target frame with three openings (one each for a bare gold foil, a lithium coated gold foil, and a quartz viewer) to be inserted down from the chamber lid into the beam in the SUNY Geneseo 15R scattering chamber. The feedthrough itself is a stainless steel tube containing a strong neodymium magnet attached to a long aluminum rod that is attached to the target frame. Another pair of magnets in a 3D printed slider outside the tube allow the magnet inside the tube to be moved and rotated, carrying the target frame along with it.

The targets were created in the same deposition chamber that has been described in previous reports [9,10,15], but the side viewport was removed to attach the airlock motion feedthrough and allow the target substrate to be inserted just above the top of the "house" and directly above the lithium boat. When the lithium boat is heated, atoms of lithium evaporate and travel upward to become deposited on the surface of the gold foil attached to a target frame. The glove bag was modified to allow the airlock feedthrough to extend outside. After the lithium was deposited on the gold, the target frame was retracted into the holder and the gate valve was closed to seal it in.

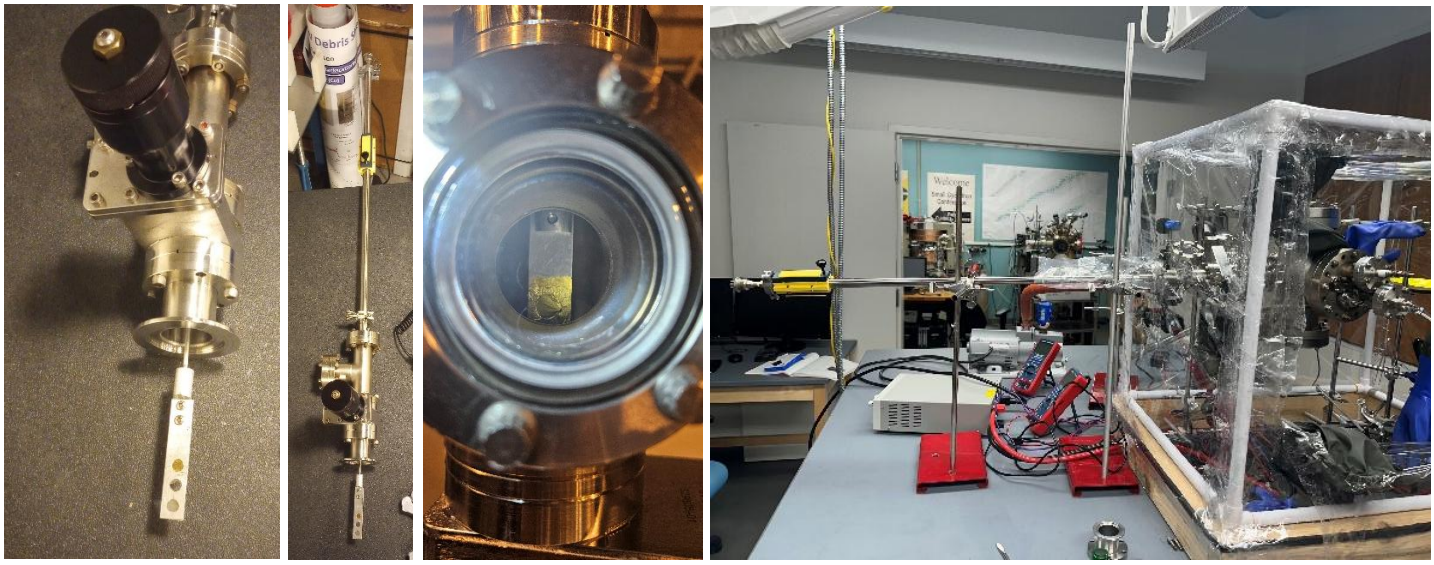

Figure 5. (From left to right) "Airlock" target holder to allow the target to be created, transported, and inserted without ever being exposed to air. High-strength neodymium magnets inside and outside the long tube allow translation and rotation of the target. The target can be pulled entirely within the tube and the gate valve closed to keep the target in a vacuum. A window allows the target foils to be viewed, and a thermocouple gauge allows the pressure inside the holder to be monitored. A mechanical roughing pump can be attached to refresh the vacuum as needed. The target holder can be attached to the side of the deposition chamber. The target substrate can be inserted in just above a hole in the "house" though which lithium ions flow upward, causing the substrate to become coated with lithium.

The entire airlock assembly was then removed from the deposition vacuum system and transported to SUNY Geneseo. Along the way, the pressure could be monitored using a hand-help battery operated thermocouple gauge controller. Once at SUNY Geneseo, the airlock assembly was attached to a forepump and re-pumped to a lower pressure. With the forepump, the pressure fell to around 30 mTorr, during the trip to Geneseo it had risen to around 100 mTorr, is a test at Houghton when stored overnight it got up to about 500 mTorr. After it was transported to Geneseo and inserted into the scattering chamber there was no detectable change in color that would indicate oxidization.

Typical targets are shown in Figure 6. Apparently, as the lithium coated the gold, the gold and lithium mixed and did not remain in separate layers. In fact, in two of the three targets that were successfully created the lithium reached all the way to the back and turned the back surface of the gold gray.

IV. Results

Measurements are still underway as this report is being written, so only a preliminary look at the data can be given, and determination of the cross sections will require more careful analysis. Figure 7 and Figure 8 show the RBS energy spectrum at 166° for 1.51 MeV deuterons. As expected, at the highest energy is the ^{6}Li(d, α)^{4}He peak, which is what will be used to measure target thickness in the future. The ^{7}Li(d,α)^{5}He reaction gives a peak at around 6.6 MeV, but this turns into a shoulder because of the three-body final state ^{7}Li(d, nα)^{4}He. The ^{6}Li(d, d)^{6}Li and ^{7}Li(d, d)^{7}Li elastic scattering peaks are indicated, but the ^{6}Li peak appears as a small bump on the side of the ^{6}Li peak. There are other peaks that may be attributable to ^{6}Li(d,p)^{7}Li and ^{7}Li(d,^{3}He)^{5}He.

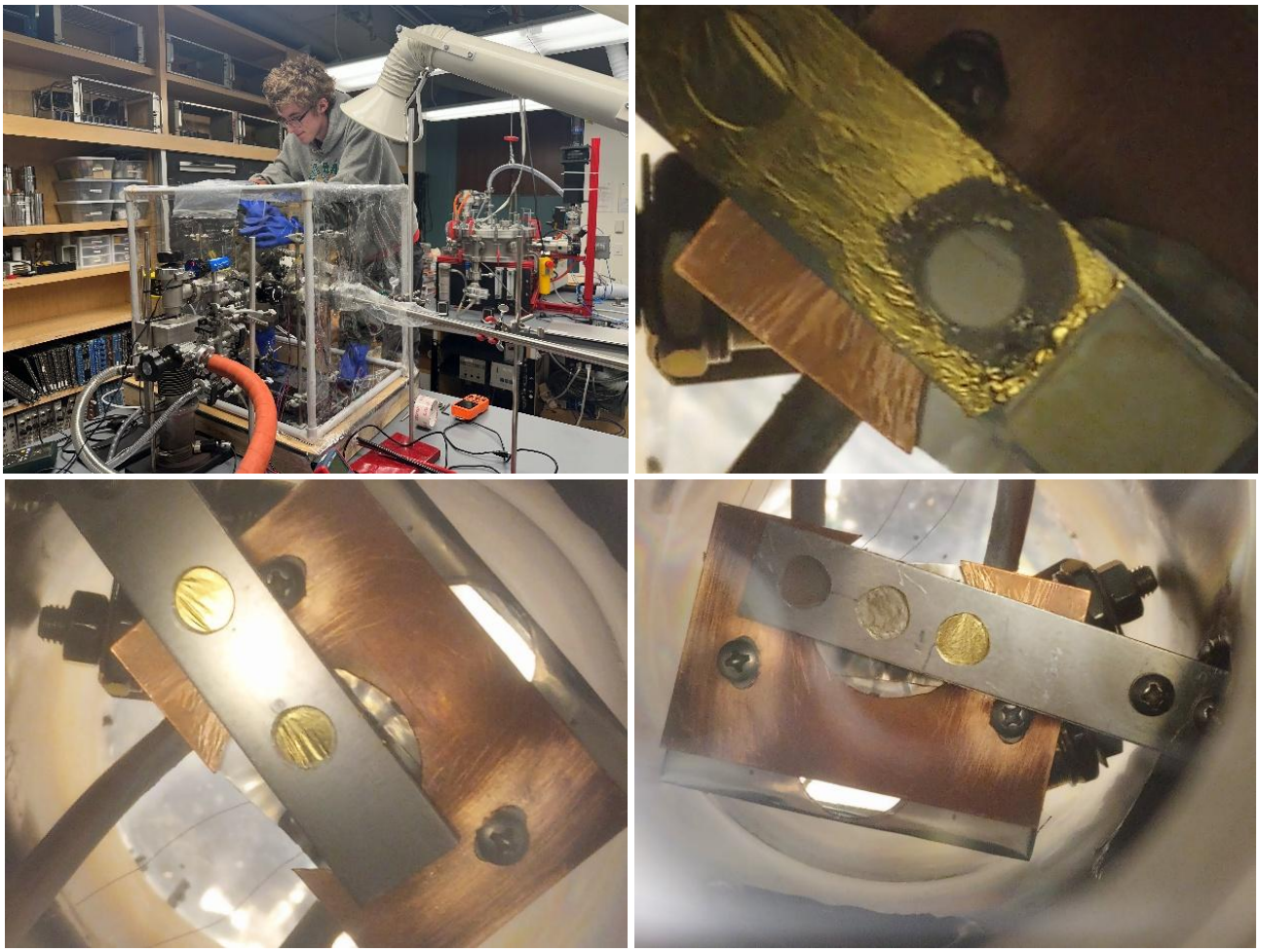

Figure 6. (Top left) Houghton University student Andrew Bo preparing the deposition chamber to make a thin Lithium target film. (Top right) A thin film of lithium (gray) was deposited on the self-supporting 116 nm thick gold foil. (Bottom left) From the RBS data it was clear that the gold and lithium mixed. In this photograph, lithium was deposited opposite the side shown, and the mixing did not reach the back surface of the gold, which remained gold colored. (Bottom right) In this photograph, the lithium penetrated all the way to the back surface of the gold. The target frame has three openings, the leftmost is a quartz viewer, the center is lithium coated gold, and the rightmost is bare gold.

The ^{197}Au(d, d) ^{197}Au elastic scattering peak is by far the largest peak and tails off at low energies much more in the lithium coated gold spectrum than the bare gold spectrum. This indicates that the gold has mixed with the lithium, with the gold density decreasing with depth into the lithium, so that the number of scattered deuterons form the surface (with higher energies) is greater than after penetrating further into the target. The impurities in the gold show up as slightly lower energy elastic scattering peaks for ^{107}Ag(d,d) ^{107}Ag, ^{105}Ag(d, d) ^{105}Ag and ^{67}Cu(d, d)^{67}Cu, as shown in Figure 9.

Figure 10 and Figure 11 show the same RBS energy spectra, but for 1.5 MeV protons. The largest peak is again elastic scattering from gold, and the highest energy peak is alpha particles from ^{7}Li(p, α)^{4}He. The ^{6}Li(p, p)^{6}Li and ^{7}Li(p, p)^{7}Li elastic scattering peaks seem to be more clearly defined than in the deuteron scattering spectra.

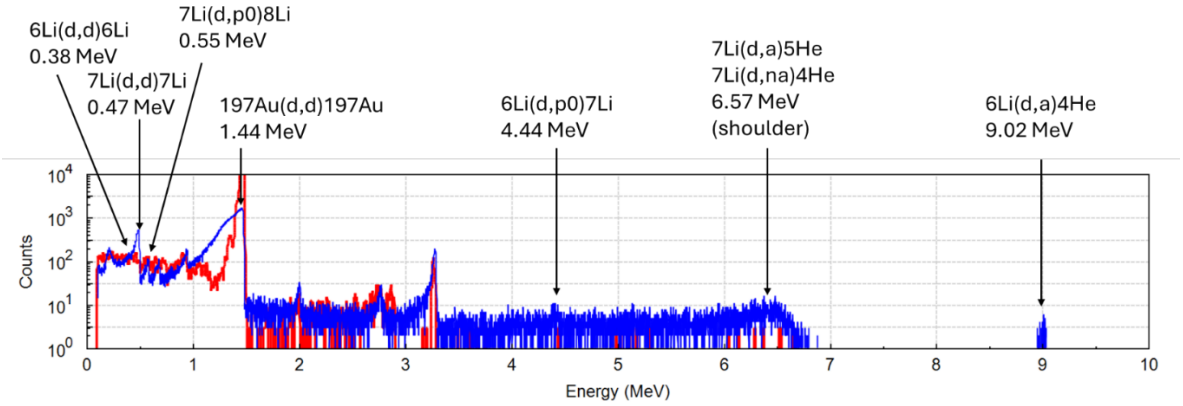

Figure 7. The energy spectrum at 166° collected by the RBS detector for 1.51 MeV deuterons incident on the bare gold target (red) and the lithium coated gold target (blue) oriented normal to the beam. Several reaction peaks of interest are labeled. From the shape of the gold peak, it is clear that the gold has migrated into the lithium. The unknown peaks at energies above 1.5 MeV seem to be associated with the gold.

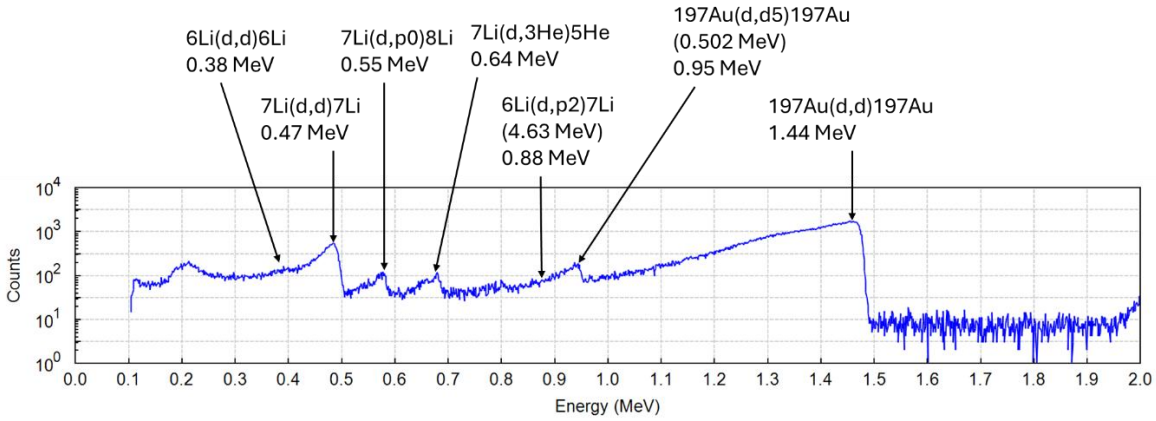

Figure 8. The region of the 166° RBS detector energy spectrum below 2 MeV for 1.51 MeV deuterons incident on the lithium coated gold target oriented normal to the beam. Preliminary assignments of reactions of interest to peaks are shown.

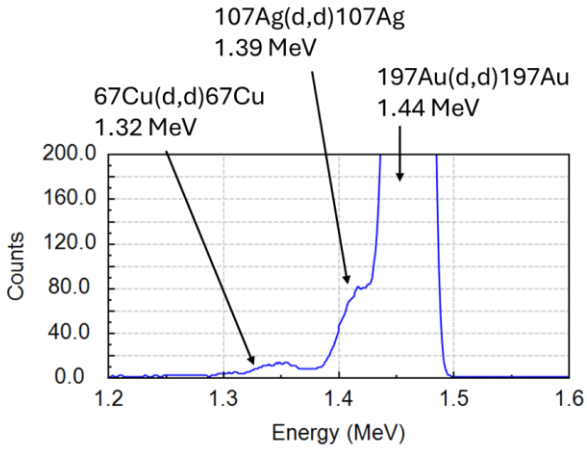

Figure 9. The region of the 166° RBS detector energy spectrum right around the gold elastic scattering peak for 1.51 MeV deuterons incident on the bare gold target oriented normal to the beam. Peaks due to silver and copper in the 24 carat gold (96% gold, 3.5% silver, and 0.5% copper) are visible.

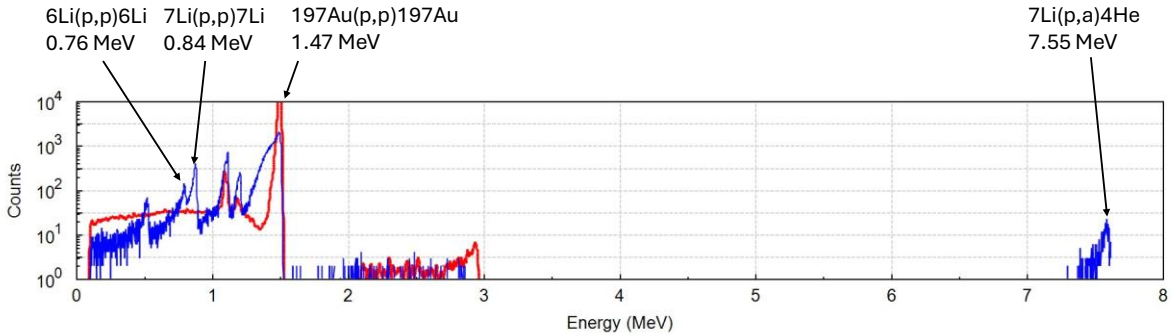

Figure 10. The energy spectrum at 166° collected by the RBS detector for 1.51 MeV protons incident on the bare gold target (red) and the lithium coated gold target (blue) oriented normal to the beam. Several reaction peaks of interest are labeled.

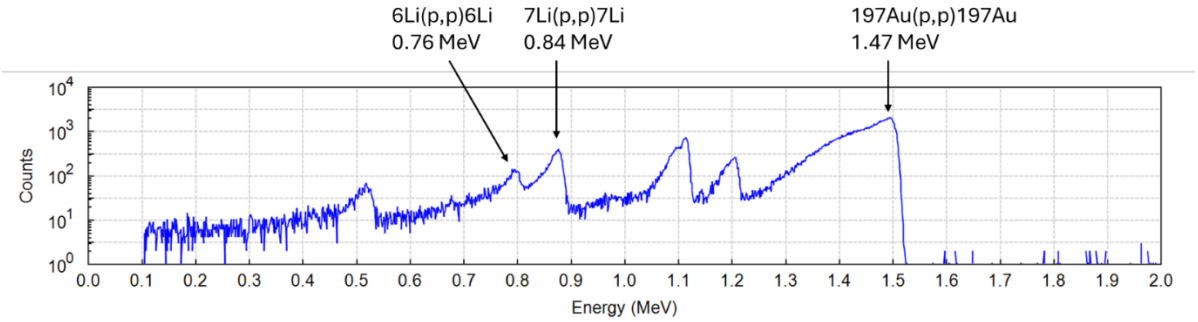

Figure 11. The region of the 166° RBS detector energy spectrum below 2 MeV for 1.51 MeV protons incident on the lithium coated gold target oriented normal to the beam. Preliminary assignments of reactions of interest to peaks are shown.

V. Future Plans

The immediate plans for this project is to continue with the data analysis in order to calculate the beam currents, lithium thickness, and eventually obtain the desired cross sections. Houghton student Dante Vara will be working on this project over the course of the upcoming academic year as part of the PHYS 371-375 Physics Project Lab sequence, which will continue for the next two years and lead to an undergraduate thesis. Our hope is this will eventually result in a publication.

The cross sections measured in this experiment will be used to reduce the uncertainty in the measurement of the SLICS efficiency in Figure 1.

VI. Talks given since summer 2024

Mark Yuly, ChunSun Lei, Andrew Martin, Stephen J. Padalino, Kurt Fletcher, Charles Freeman, George Marcus, Chad J. Forrest, Ben Stanley, Christian Stoeckl, Chad Mileham, Arnold Schwemmlein, and Sean P. Regan, "**Nuclear Physics using Ultrafast High-Power Laser Ion Acceleration,"** 66th Annual Meeting of the APS Division of Plasma Physics, Atlanta, GA, October 7-11, 2024. (https://dspace.houghton.edu/handle/hc/4216)

VII. Posters presented since summer 2024

Andrew Bo, Avery Belanger, Owen Fall, Mark Yuly, Shoshanna Hertz, Silas Richardson, Liam Wilson, Delvin Ramos, Michelle Woods, Stephen J. Padalino, Kurt Fletcher, Charles Freeman, George Marcus, Chad J. Forrest, and Sean P. Regan, **"Test of GEANT 4 Simulation Efficiency Predictions for the Short-lived Isotope Counting System,"** 16th OMEGA Laser User's Group Meeting, Laboratory for Laser Energetics,

Rochester, NY, May 21, 2025; 66th Annual Meeting of the APS Division of Plasma Physics, Atlanta, GA, October 7-11, 2024. (https://dspace.houghton.edu/handle/hc/4215)

Andrew Bo, Avery Belanger, Owen Fall, Mark Yuly, Stephen J. Padalino, Kurt Fletcher, Charles Freeman, and George Marcus, Chad J. Forest, Ben Stanley, and Sean P. Regan, **"Detecting Short-lived Isotopes Outside the OMEGA-60 Target Chamber Milliseconds After a High-Yield Shot,"** 16th OMEGA Laser User's Group Meeting, Laboratory for Laser Energetics, Rochester, NY, May 21, 2025; 66th Annual Meeting of the APS Division of Plasma Physics, Atlanta, GA, October 7-11, 2024. (https://dspace.houghton.edu/handle/hc/4214)

This material is based upon work supported by the Department of Energy [National Nuclear Security Administration] University of Rochester "National Inertial Confinement Program" under Award Number(s) DE-NA0004144.

---

[1] Katelyn Cook, B.S. thesis, (Houghton College, 2019).

[2] Mark Yuly, Stephen Padalino, Micah Coates and Katelyn Cook, "A possible measurement of the 3H(t,γ)6He cross section at low energy," in Nuclear and Plasma Diagnostics for the EP-OMEGA and MTW Laser Systems, LLE Proposal for Subaward 416231-G (2016) (unpublished).

[3] Mark Yuly, Stephen Padalino, Micah Coates and Katelyn Cook, "A Phoswich Detector System to Measure the $^{3}H(t,\alpha)^{6}He$ Cross Section using ICF" in Nuclear and Plasma Diagnostics for the EP-OMEGA and MTW Laser Systems, LLE Proposal for Subaward 416231-G (2017) (unpublished).

[4] Mark Yuly, Stephen Padalino, Emma Bruce, Katelyn Cook, and Sarah Hull, "Measuring Low Energy Nuclear Cross Sections using ICF," in Nuclear and Plasma Diagnostics for the EP-OMEGA and MTW Laser Systems, LLE Proposal for Subaward 416231-G (2018) (unpublished).

[5] Mark Yuly, Stephen Padalino, Tyler Kowalewski, Salvatore Ferri and Steven Raymond, "Inertial Confinement Fusion as a Tool to Study Fundamental Nuclear Science," in Nuclear and Plasma Diagnostics for the EP-OMEGA and MTW Laser Systems, LLE Proposal for Subaward 416231-G (2019) (unpublished).

[6] Mark Yuly, Stephen Padalino, Micah Christensen, Joshua Bowman, "Progress toward using ICF to measure light-ion nuclear cross sections" in Nuclear and Plasma Diagnostics for the EP-OMEGA and MTW Laser Systems, LLE Proposal for Subaward 416231-G (2020) (unpublished).

[7] Mark Yuly, Stephen Padalino, Adam Brown, Micah Christensen, Micah Condie, "Trapping and detecting trace radioactive isotopes produced in ICF implosions," in Nuclear and Plasma Diagnostics for the EP-OMEGA and MTW Laser Systems, LLE Proposal for Subaward 416231-G (2021) (unpublished).

[8] Tyler Kowalewski, “Inertial Confinement Fusion as a Tool to Study Fundamental Nuclear Science,” B.S. Thesis (Houghton College, 2021).

[9] Mark Yuly, Stephen Padalino, Adam Brown, Andrew Hotchkiss, Chunsun Lei, Andrew Martin. “Trapping and detecting trace radioactive isotopes produced in ICF implosions,” in Nuclear and Plasma Diagnostics for the EP-OMEGA and MTW Laser Systems, LLE Proposal for Subaward 416231-G (2022) (unpublished).

[10] Mark Yuly, Stephen Padalino, Noah Harley, Andrew Hotchkiss, Chunsun Lei, Andrew Martin. “A new technique for measuring light ion nuclear reactions using TNSA,” in Nuclear and Plasma Diagnostics for the EP-OMEGA and MTW Laser Systems, LLE Proposal for Subaward 416231-G (2023) (unpublished).

[11] Andrew Martin, B.S. thesis, (Houghton College, 2023).

[12] Mark Yuly, Andrew Bo, Avery Belanger, Owen Fall, Stephen Padalino, and Charlie Freeman. “Nuclear physics using ultrafast high-power laser ion acceleration,” in Nuclear and Plasma Diagnostics for the EP-OMEGA and MTW Laser Systems, LLE Proposal for Subaward 416231-G (2024) (unpublished).

[13] M. Bikchurina, Proceedings of ISINN-29, JINR, E3-2023-58, Dubna, 2023, p.75 – 87.

[14] M. Mayer. SIMNRA User’s Guide. Tech. rep. IPP 9/113. Garching: Max-Planck-Institut für Plasmaphysik, 1997.

[15] Chunsun Lei, B.S. thesis, (Houghton College, 2023).